arXiv:quant-ph/0310096v5 10 Feb 2008

# A quantum trajectory description of decoherence

A. S. Sanz[1] and F. Borondo[2]

[1] Instituto de Matemáticas y Física Fundamental, Consejo Superior de Investigaciones Científicas, Serrano 123, 28006 Madrid, Spain

[2] Departamento de Química, C–IX, Universidad Autónoma de Madrid, Cantoblanco – 28049 Madrid, Spain

**Abstract.** A complete theoretical treatment in many problems relevant to physics, chemistry, and biology requires considering the action of the environment over the system of interest. Usually the environment involves a relatively large number of degrees of freedom, this making the problem numerically intractable from a purely quantum–mechanical point of view. To overcome this drawback, a new class of quantum trajectories is proposed. These trajectories, based on the same grounds as Bohmian ones, are solely associated to the system reduced density matrix, since the evolution of the environment degrees of freedom is not considered explicitly. Within this approach, environment effects come into play through a time–dependent damping factor that appears in the system equations of motion. Apart from their evident computational advantage, this type of trajectories also results very insightful to understand the system decoherence. In particular, here we show the usefulness of these trajectories analyzing decoherence effects in interference phenomena, taking as a working model the well–known double–slit experiment.

**PACS.** 03.65.-w Quantum mechanics (general) – 03.65.Ta Foundations of quantum mechanics; measurement theory – 03.65.Yz Decoherence; open systems; quantum statistical methods – 03.75.Dg Atom and neutron interferometry

## 1 Introduction

Among the different alternative mechanisms proposed to explain how the behavior of a quantum system becomes classical–like [1], decoherence is the most widely accepted [2,3]. Decoherence is the irreversible emergence of classical properties when an isolated system, namely the system of interest, interacts with an environment [4]. The environment can be constituted by many randomly distributed particles interacting with the system by means of scattering processes. When these events occur in a large number, the off–diagonal elements of the system reduced density matrix undergo an exponential damping [5], this making the system to quickly lose its coherence. Coherence loss is an important issue, for example, in quantum computation [6], where long chains of atoms must be kept in a coherent superposition for certain time in order to perform the corresponding operations. Therefore, decoherence effects must be considered seriously; they increase rapidly with the length of the chain [7], thus decreasing the efficiency of the latter in performing such operations.

At a first glance, Bohmian mechanics (BM) [8,9] seems to be a suitable tool to study and shed light on decoherence problems. Unlike the standard version of quantum mechanics (SQM), the Bohmian formalism is based on the concept of well–defined trajectories; particles are always regarded as particles, as in classical mechanics. The particle motion, governed by the wave function, leads to the same results provided by SQM when a sampling over particle initial conditions is considered (see, for example, reference [10]). This capability to conjugate motion and statistical predictions within a purely quantum framework has been widely used to describe, for example, interference experiments with slits [11,12,13,14,15,16], where decoherence can play an important role.

Nevertheless, despite the apparent suitability of BM to the study of decoherence, in practice its application results numerically prohibitive in problems where the number of degrees of freedom involved becomes relatively large. To overcome this computational drawback one can proceed as in SQM when dealing with Markovian environments [17]. In these cases, decoherence effects can be studied by using a master equation formulation, where the particular time–evolution of the different environment degrees of freedom is not taken into account explicitly. The Markovian master equation, derived from the von Neumann equation for the whole system (the system of interest plus the environment), is generally expressed as a sum of two contributions, which are responsible for: (1) the time–evolution of the isolated system, and (2) the quenching leading to the system coherence loss. All the information regarding the physical properties of the environment as well as its interaction with the system is contained within this second term.

Starting from BM, one can proceed as in SQM and consider the "average" action of the environment degrees

of freedom in order to obtain a Markovian–like trajectory equation of motion. We can thus define a *new* class of quantum trajectories, the *reduced quantum trajectories*, directly related to the system reduced density matrix, but also influenced by the presence of the environment. Within this formulation, the environment degrees of freedom come into play through a time–dependent damping factor that appears in the expression for the particle velocity field. Avoiding to integrate explicitly the equations of motion for the environment degrees of freedom allows to obtain an important insight on the system dynamics at a low computational cost.

To illustrate the applicability and interest of the reduced quantum trajectories, we will use them to analyze the effects of decoherence in interference phenomena. These phenomena constitute an ideal framework to study decoherence because of their simplicity as well as their fundamental implications in quantum mechanics. In particular, we will focus our discussion on the double–slit experiment, which can be regarded as the paradigm of quantum interference. In this experiment, in the absence of "which–way" information, the measured intensity displays the well–known interference pattern with maximum fringe visibility. On the other hand, the knowledge of the particle pathway destroys such a pattern and the intensity thus acquires classical features, i.e., it is simply given by the sum of the intensities corresponding to each pathway[1]. These two possible outcomes[2], related to which aspect of the particle we are interested in (wave or corpuscle, respectively), are equivalent to consider two different experimental contexts: both slits simultaneously open or each one independently open. The choice of a quantum context determines the intensity pattern, in sharp contrast to what happens in classical mechanics in the analogous situation, where both contexts give the same result. However, if the action of an external environment (air molecules, thermal photons, etc.) over the system is taken into account between the slits and the detector, a partial (or even total) suppression of the quantum interference will be observed in the intensity pattern. This means that a certain amount of "which–way" information is being gradually revealed, and the process can be thought as a smooth transition from the context where both slits are simultaneously open to the other one where they are independently open.

The organization of this paper is as follows. In Section 2 we introduce the formal grounds of the reduced quantum trajectory formalism as well as its theoretical application to the double–slit problem. In Section 3 we present an application of this formalism to the double–slit experiment with cold neutrons performed by Zeilinger *et al.* [20]. Finally, in Section 4 the main conclusions arisen from this work are summarized.

[1] Except otherwise stated, throughout this work "classical" refers to the lack of quantum interference, though in general this does not mean necessarily lack of other quantum effects (e.g., single–slit diffraction [14]).

[2] Though in SQM textbooks these two situations are mutually exclusive, it has been shown both theoretically [18] and experimentally [19] that it is still possible to determine certain amount of "which–way" information without a full erasure of the interference pattern.

## 2 Decoherence and quantum trajectories

### 2.1 The reduced quantum trajectory approach

In order to extract useful information about the system of interest, one usually computes its associated reduced density matrix by tracing the total density matrix[3], $\hat{\rho}_t$, over the environment degrees of freedom. In the configuration representation and for an environment constituted by $N$ particles, the system reduced density matrix is obtained after integrating $\hat{\rho}_t \equiv |\Psi\rangle_t\, {}_t\langle\Psi|$ over the $3N$ environment degrees of freedom, $\{\mathbf{r}_i\}_{i=1}^N$,

$$\tilde{\rho}_t(\mathbf{r},\mathbf{r}') = \int \langle \mathbf{r},\mathbf{r}_1,\mathbf{r}_2,\ldots\mathbf{r}_n|\Psi\rangle_t \times {}_t\langle\Psi|\mathbf{r}',\mathbf{r}_1,\mathbf{r}_2,\ldots\mathbf{r}_n\rangle\, \mathrm{d}\mathbf{r}_1\mathrm{d}\mathbf{r}_2\cdots\mathrm{d}\mathbf{r}_n. \quad (1)$$

The system (reduced) quantum density current can be derived from this expression [21,22], being

$$\tilde{\mathbf{J}}_t \equiv \frac{\hbar}{m}\, \mathrm{Im}[\nabla_{\mathbf{r}}\tilde{\rho}_t(\mathbf{r},\mathbf{r}')]\Big|_{\mathbf{r}'=\mathbf{r}}, \quad (2)$$

which satisfies the continuity equation

$$\dot{\tilde{\rho}}_t + \nabla\tilde{\mathbf{J}}_t = 0. \quad (3)$$

In equation (3), $\tilde{\rho}_t$ is the diagonal element (i.e., $\tilde{\rho}_t \equiv \tilde{\rho}_t(\mathbf{r},\mathbf{r})$) of the reduced density matrix and gives the measured intensity [23].

Taking into account equations (2) and (3), now we define the velocity field, $\dot{\mathbf{r}}$, associated to the (reduced) system dynamics as

$$\tilde{\mathbf{J}}_t = \tilde{\rho}_t\dot{\mathbf{r}}, \quad (4)$$

which is analogous to the Bohmian velocity field. Now, from equation (4), we define a new class of quantum trajectories as the solutions to the equation of motion

$$\dot{\mathbf{r}} \equiv \frac{\hbar}{m}\frac{\mathrm{Im}[\nabla_{\mathbf{r}}\tilde{\rho}_t(\mathbf{r},\mathbf{r}')]}{\mathrm{Re}[\tilde{\rho}_t(\mathbf{r},\mathbf{r}')]}\Bigg|_{\mathbf{r}'=\mathbf{r}}. \quad (5)$$

These new trajectories are related to the system reduced density matrix, therefore we call them the *reduced quantum trajectories*. In Section 3 we will see that the dynamics described by equation (5) leads to the correct intensity (whose time–evolution is described by equation (3)) when the statistics of a large number of particles is considered. Moreover, also observe that equation (5) reduces to the well–known expression for the velocity field in BM when there is no interaction with the environment. This can be shown as follows. The decoupling from the environment

[3] Throughout this work, we indicate time–dependence by a subscript "$t$" (e.g., $\hat{\rho}_t \equiv \hat{\rho}(t)$), while initial values do not carry any label (e.g., $\hat{\rho} \equiv \hat{\rho}(0)$).

makes the system reduced density matrix to be just the system density matrix. Making then use of the BM ansatz for the system wave function ($\langle \mathbf{r}|\Psi\rangle_t = R_t(\mathbf{r})\, e^{iS_t(\mathbf{r})/\hbar}$), we can express the system density matrix as

$$\rho_t(\mathbf{r},\mathbf{r}') = R_t R_t'\, \mathrm{e}^{i(S_t - S_t')/\hbar}, \tag{6}$$

with $R_t' = R_t(\mathbf{r}')$ and $S_t' = S_t(\mathbf{r}')$. Finally, substituting (6) into equation (5), one reaches

$$\dot{\mathbf{r}} = \frac{\nabla S_t}{m}, \tag{7}$$

which, effectively, is the well–known expression for the particle equation of motion in BM.

As mentioned above, BM becomes numerically intractable when the phenomena described involve a large number of degrees of freedom. Hence a wide range of alternative, approximate formulations rooted in this approach have been proposed in the literature [24]. The reason behind formulating these alternative formalisms is quite simple. BM is the only trajectory–based approach compatible with SQM where no approximations are considered, this leading to a straightforward interpretation of quantum phenomena in terms of a self–consistent quantum theory of motion (all the elements contained in the theory are ruled by quantum laws). Therefore any approximation to BM will also remain relatively close to SQM, reducing at the same time the computational efforts implicated by many degree–of–freedom systems. As we have seen, these features also meet in our approach, whose mathematical structure remains very close to that of BM.

Nevertheless, the aforementioned formulations are not so widespread as those other based on the so–called semiclassical approximation of the wave function, in particular, the semiclassical initial value representation (SC–IVR) [25], which is one of the most successful approaches to date. Unlike the previous prescriptions, the self–consistency mentioned above breaks in SC–IVR schemes: on the one hand we have the calculation of purely classical trajectories; on the other hand, there is a (semiclassical) wave function which is calculated from those classical trajectories.

The intertwining between classical and quantum mechanics in a Feynman–like fashion [15,26] constitutes the main difference with respect to Bohmian–like schemes, such as the one described in this work. This difference can be noticed, for instance, when looking at the dynamics displayed by the trajectories representative of each type of formalism. In semiclassical approaches trajectories will be just classical, not showing any particular effect typical of the quantum problem treated with them; only when these trajectories are introduced into the semiclassical wave function a quantum description of the phenomenon that we are dealing with can be obtained. On the contrary, in Bohmian–like schemes, the trajectories display a topology that is in accordance (in a more or less degree, depending on the approximation considered) with the dynamics prescribed by quantum laws. In other words, even considering the same initial condition for both types of trajectories the differences between the motions described by each one will manifest immediately. This comparison can be seen in reference [15], where classical and Bohmian trajectories were obtained within the context of the double–slit experiment with no coupling to an environment (calculations applying the SC–IVR formalism to the double–slit experiment can be seen in references (e) and (f) in [25], for example, but no classical trajectories related were explicitly shown).

### 2.2 Reduced trajectory dynamics in the double–slit experiment

The implications and usefulness of equation (5) are better appreciated when analyzing decoherence effects in the double–slit experiment. Quantum mechanically the evolution of a particle after passing through a double–slit setup (and without being acted by an external environment) can be described at any subsequent time by a wave function

$$|\Psi^{(0)}\rangle_t = c_1|\psi_1\rangle_t + c_2|\psi_2\rangle_t, \tag{8}$$

where $|\psi_j\rangle_t$ is the partial wave emerging from the slit $j$ (with $j = 1,2$), and $|c_1|^2 + |c_2|^2 = 1$ at any time. In configuration space, the density matrix associated to the wave function (8) is

$$\rho_t^{(0)}(\mathbf{r},\mathbf{r}') = \Psi_t^{(0)}(\mathbf{r}) \left[\Psi_t^{(0)}(\mathbf{r}')\right]^*, \tag{9}$$

with $\Psi_t^{(0)}(\mathbf{r}) = \langle \mathbf{r}|\Psi^{(0)}\rangle_t$. As said above, the diagonal of equation (9) gives the measured intensity (or probability density),

$$\rho_t^{(0)}(\mathbf{r}) = |c_1|^2|\psi_1|_t^2 + |c_2|^2|\psi_2|_t^2 + 2|c_1||c_2||\psi_1|_t|\psi_2|_t \cos\delta_t \tag{10}$$

where $\delta_t$ is the time–dependent phase shift between the partial waves.

Under the presence of an environment, the wave function (8) does no longer describe the evolution of the isolated system. To obtain an appropriate ansatz, first we consider elastic system–environment scattering conditions, which lead to a gradual suppression of the interference terms in equation (10) without changing too much the states describing the system (i.e., each partial wave). Under these conditions, only the environment states, $|E_j\rangle_t$, associated with each partial wave will change during the scattering process. In addition, we also assume that the system is initially represented by a superposition of two Gaussian wave packets (see Section 3); both partial waves will then keep their Gaussian shape during their time–evolution, this simplifying the analysis of the problem. Taking this into account, a general initial separable coherent state

$$|\Psi\rangle = |\Psi^{(0)}\rangle \otimes |E_0\rangle \tag{11}$$

(with $|\Psi^{(0)}\rangle$ as in equation (8) at $t = 0$) will become entangled,

$$|\Psi\rangle_t = c_1|\psi_1\rangle_t \otimes |E_1\rangle_t + c_2|\psi_2\rangle_t \otimes |E_2\rangle_t, \tag{12}$$

at any subsequent time. Let us recall that the condition of initial coherence also means that $|E_1\rangle = |E_2\rangle = |E_0\rangle$ at $t = 0$.

Provided elastic system–environment scattering conditions as well as weak interactions are assumed the decoherence process can be described by means of (12). However, this assumption will no longer be valid as the system–environment coupling becomes stronger and energy transfer inelastic processes take place. Such processes would imply a more complicated form for the wave function, which could not be expressed in terms of two overlapping, spreading Gaussians. Instead, the energy transfer leads not only to a change of the shape of the diffracted beams, but, more importantly, to a mixed state that cannot be described in general as a simple wave function due to the strong intertwining between the environment states and the system ones. In such cases, one should to consider either the language of density matrices commonly used in the theory of open quantum systems [17,27], or the stochastic wave functions that appear in the quantum state diffusion prescription [28].

The effects induced by strong couplings can be better appreciated, for instance, when using the SC–IVR formalism mentioned above, where the environment is characterized by a certain spectral density of frequencies (in general the environment is assumed to be a bath harmonic oscillators with an Ohmic spectral density). The aforementioned intertwining between environment and system states leads to a very appealing loss of interferences in both bound systems (e.g., vibrating diatoms in solvents; see reference (d) in [25]) and problems in the continuum (e.g., inelastic scattering of He atoms from a Cu surface; see reference (g) in [25]). Nonetheless, as the coupling strength increases more, this type of descriptions may also lose their validity, since the bath of harmonic oscillators will not longer describe properly the system–environment coupling, which could be more complicated and lead to dissipation.

From (12) the measured intensity is obtained from the system reduced density matrix, which is given by the trace of the full density matrix over the environment states,

$$\hat{\tilde{\rho}}_t = \sum_{j=1}^{2} {}_t\langle E_j|\hat{\rho}_t|E_j\rangle_t \tag{13}$$

(notice that this expression is equivalent to (1)). Thus, substituting the wave function (12) in equation (13) gives

$$\tilde{\rho}_t(\mathbf{r},\mathbf{r}') = (1+|\alpha_t|^2)\sum_{j=1}^{2}|c_j|^2\psi_{j,t}(\mathbf{r})\psi^*_{j,t}(\mathbf{r}') + 2\alpha_t c_1 c_2^* \psi_{1t}(\mathbf{r})\psi^*_{2t}(\mathbf{r}') + c.c., \tag{14}$$

where $\alpha_t \equiv {}_t\langle E_2|E_1\rangle_t$ and *c.c.* means conjugate complex, and from this expression the measured intensity results

$$\tilde{\rho}_t = (1+|\alpha_t|^2)\left[|c_1|^2|\psi_1|_t^2 + |c_2|^2|\psi_2|_t^2 + 2\Lambda_t|c_1||c_2||\psi_1|_t|\psi_2|_t\cos\delta_t'\right], \tag{15}$$

with

$$\Lambda_t \equiv \frac{2|\alpha_t|}{(1+|\alpha_t|^2)} \tag{16}$$

being the *coherence degree*, which gives the value of the *fringe visibility* in a good approximation [23]. For the sake of simplicity, we have assumed that the phase difference between the environment states (included in $\delta_t'$) is constant.

The environment states are considered to be too complicated for keeping mutual coherence as time increases [29]; even if they are initially coherent, they will become orthogonal along time. Thus, one can assume $|\alpha_t| = \mathrm{e}^{-t/\tau_c}$, $\tau_c$ being the coherence time, a measure of how fast the system looses its coherence. Introducing this value into equation (16), we obtain

$$\Lambda_t = \mathrm{sech}(t/\tau_c), \tag{17}$$

which establishes a relationship between the coherence degree and the coherence time. Thus, although the value of the coherence time can be derived analytically for interfering waves by means of simple Markovian models [30], equation (17) allows us to determine it from the empirical value of $\Lambda_t$ [23] (i.e., measured from the intensity pattern) and the time–of–flight, $t_f$, of the diffracted particles. Because of the empirical nature of $\tau_c$ (or, equivalently, the value of $\Lambda_t$ after a full flight) in our model, temperature does not appear explicitly despite its important role in decoherence phenomena. Within the context of the double–slit experiment, this issue has been treated in some theoretical [30,31] and computational (references (e) and (f) in [25]) works in the literature. In this way, following references [30,31], $\tau_c$ would already encompass the effects of the temperature. Note that this dependence on temperature is quite different from that in semiclassical treatments; in the first case it is simply a parameter, where in the latter it appears as a consequence of considering the bath of oscillators at the equilibrium at a given temperature (i.e., the oscillators follow a Boltzmann distribution).

As said above, equation (5) has been defined in such a way that there is no an explicit dependence on the dynamical evolution of the environment degrees of freedom. Nevertheless, the environment effects on the system will still be present through $\alpha_t$, as seen when substituting (14) into equation (5). This can be seen in the resulting equation of motion

$$\dot{\mathbf{r}}_t = \frac{(1+|\alpha_t|^2)\hbar}{2im\tilde{\rho}_t}\sum_{j=1}^{2}|c_j|^2\left[\psi^*_{j,t}\nabla\psi_{j,t} - \psi_{j,t}\nabla\psi^*_{j,t}\right] + \frac{\hbar}{im\tilde{\rho}_t}\alpha_t c_1 c_2^*\left[\psi^*_{2,t}\nabla\psi_{1,t} - \psi_{1,t}\nabla\psi^*_{2,t}\right] + c.c. \tag{18}$$

In the limit of total loss of coherence (i.e., $t \gg \tau_c$ or $\alpha_t \to 0$), equation (18) becomes

$$\dot{\mathbf{r}}_t = \frac{|c_1|^2\rho_t^{(1)}\dot{\mathbf{r}}_1 + |c_2|^2\rho_t^{(2)}\dot{\mathbf{r}}_2}{\rho_t^{\mathrm{cl}}} \tag{19}$$

where $\dot{\mathbf{r}}_j$ and $\rho_t^{(j)}$ are, respectively, the velocity field and the probability density associated to the partial wave $|\psi_j\rangle_t$, and

$$\rho_t^{\mathrm{cl}} \equiv |c_1|^2\rho_t^{(1)} + |c_2|^2\rho_t^{(2)}. \tag{20}$$

Notice that both $\rho_t^{\rm cl}$ and the density current,

$$\mathbf{J}_t^{\rm cl} \equiv \rho_t^{\rm cl}\ \dot{\mathbf{r}}_t = |c_1|^2 \rho_t^{(1)}\ \dot{\mathbf{r}}_1 + |c_2|^2 \rho_t^{(2)}\ \dot{\mathbf{r}}_2, \qquad (21)$$

are properly defined in this limit; the former is a sum of partial probability densities and the latter is the sum of the density currents corresponding to each slit independently considered. Moreover, in both cases these magnitudes are properly weighted with the coefficients $|c_1|^2$ and $|c_2|^2$. Thus, from a SQM point of view, an experiment with full decoherence is equivalent to another one performed with each slit independently open. Something different happens, however, when this situation is studied in terms of reduced quantum trajectories. In this case, particles still move under the guidance of both partial waves although interference has already disappeared. This is because the damping describing interference suppression does not account for the erasure of the information about the initial presence of two slits.

It is important to note that within a purely BM approach the limit discussed above has to be such that the corresponding Bohmian trajectories will behave as unaware of the existence of a double–slit. That is, particles started with initial conditions in one of the slits will evolve with basically no information about the presence of the other slit. Since Bohmian trajectories cannot pass through the same point in configuration space at the same time, such behavior can be explained having in mind that the trajectories describing the system–plus–environment interaction are embedded in a $3(N+1)$–dimensional configuration space. In this sense, as the system–plus–environment interaction takes place, the topology of these $3(N+1)$–dimensional trajectories will be such that the projection of the system degrees of freedom onto the system subspace will display crossings (at the same time). Of course, this does not violate the single–valuedness condition of BM, since crossings are only present in the projections. Somehow this situation resembles what happens in classical mechanics, where trajectories can pass through the same point of the configuration space at the same time, but not in phase space. Within our quantum–trajectory approach single–valuedness preserves; once the dynamics of the environment degrees of freedom is not considered explicitly, the single–valuedness condition directly emerges in the system subspace.

## 3 Decoherence in the double–slit experiment

### 3.1 Model and simulation conditions

The working model used here is based on the double–slit experiment performed by Zeilinger *et al.* with cold neutrons [20], which has also been analyzed elsewhere by us from both an optical and a SQM point of view [23]. Following the prescription given in Section 2, our simulation models the behavior of the neutron beam from the two slits to the detector. The double–slit arrangement has dimensions $a_1$–$d'$–$a_2$ = 21.9–104.1–22.5 $\mu$m (left slit/gap/right slit), and is at a distance $L = 5$ m from the detector. The wavelength of the incident neutron beam is $\lambda_{\rm dB} = 18.45$ Å, corresponding to a subsonic velocity, $v = 214.4$ m/s.

Here interference is described by considering two Gaussian slits on the $xy$–plane, with neutrons propagating along the $z$–direction. As seen in [15,23], Gaussian slits reproduce fairly well the real experiment, avoiding at the same time single–slit diffraction features [14]. To further simplify, we have assumed $\ell_y \gg \ell_x$, with $\ell_x$ and $\ell_y$ being the dimensions of the slits. This allows us to neglect the motion along the $y$–direction due to translational invariance (thus describing the particle motion only along the $x$ and $z$ coordinates). With this, $|\Psi^{(0)}\rangle$ in (11) is given by a coherent superposition of two Gaussian wave packets (here we consider that both contribute equally, i.e., $c_1 = c_2 = 1/\sqrt{2}$), each one described by

$$\psi_j(x,z) = \left(\frac{1}{2\pi\sigma_{x_j}\sigma_{z_j}}\right)^{1/2} {\rm e}^{-(x-x_j)^2/4\sigma_{x_j}^2 + ip_{x_j}x/\hbar} \times {\rm e}^{-(z-z_j)^2/4\sigma_{z_j}^2 + ip_{z_j}z/\hbar}, \qquad (22)$$

with $j = 1, 2$. Regarding the initial environment state, it is chosen as $|E_0\rangle = |\,\mathbb{I}\,\rangle$, such that $|\Psi\rangle = |\Psi^{(0)}\rangle \otimes |\,\mathbb{I}\,\rangle$.

The time evolution of the (system) partial waves is carried out numerically by Heller's method [14], which is exact in our case because there is no external potential. In the calculations, the Gaussian wave packets have been centered at $x_{1,2} = (a_{1,2} \mp d)/2$ and $z_{1,2} = 0$, and incoherence has been introduced by taking into account different propagation velocities for each wave packet [23], given by $p_{x_{1,2}} = \mp\hbar/a_{1,2}$ and $p_{z_{1,2}} = \sqrt{(2\pi\hbar/\lambda_{\rm dB})^2 - p_{x_{1,2}}^2}$. In order to minimize the spreading of the Gaussians along the $z$–direction,

$$\sigma_t^z = \sigma\sqrt{1 + \left(\frac{\hbar t}{m\sigma^2}\right)^2}, \qquad (23)$$

during the time propagation, we have chosen $\sigma = 2\bar{a}$ (with $\bar{a} = (a_1 + a_2)/2$) for both wave packets. This ensures $\sigma_t^z \simeq \sigma$ for the whole propagation time. As for the spreading along the $x$–direction, we have considered $\sigma_{x_j} = a_j/4$, so that for $|x - x_j| = a_j/2$ the intensity at the edge of slit $j$ amounts to $|\psi_j(\pm a_j/2)|^2/|\psi_j(0)|^2 = e^{-2}$ (about 13.5% of the maximum value of the intensity, $|\psi_j(0)|^2$, reached when $x = x_j$). In this way, only a very small portion of the partial waves is out of the boundaries defined by the edges of the slits. This assumption is in good agreement with the error on the slit widths experimentally reported in [20], according to which neutrons penetrating through the boron wire (the physical gap between the two slits) undergo a relatively strong attenuation.

According to Heller's propagation method, both partial waves are evolved independently. Then the parameter $\alpha_t$ is introduced whenever they are superposed in order to obtain the intensity (15). The magnitude of $|\alpha|_t$ was empirically determined in [23] taking into account the coherence degree of the experimental results ($\Lambda_t = 0.632$) and the time–of–flight of neutrons ($t_f = v/L = 2.33\times10^{-2}$ s), resulting a value of 0.36. This value implies a coherence

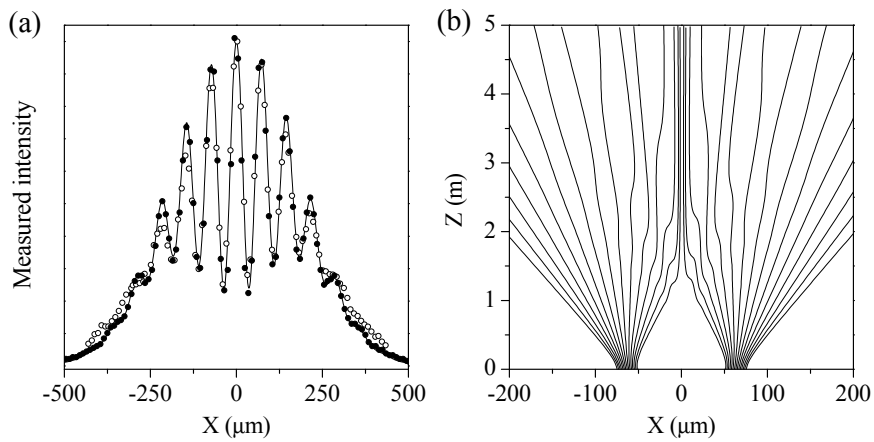


**Fig. 1.** (a) Comparison between experimental data (○) and the intensity obtained from quantum trajectory (●) and SQM (full line) calculations for a double–slit experiment with cold neutrons [20]. (b) Sample of trajectories illustrating the dynamics of the results shown in part (a).

time $\tau_c = 2.26\times10^{-2}$ s, slightly smaller than the time–of–flight.

The reduced quantum trajectories were integrated according to equation (18) at the same time that the partial waves were propagated. To obtain the statistical results, about 5,420 trajectories were used in each calculation shown below, binning them in space intervals of 20 $\mu$m, which coincides with the experimental scanning slit width [20]. These trajectories were initially distributed according to the probability density $\rho^{(0)}$, thus ensuring the agreement with SQM calculations through equation (3).

### 3.2 Numerical results

In Figure 1(a) the results obtained from the statistics of trajectories (●) are plotted together with the experimental values (○). Also to compare, we have included the results from SQM (solid line), as given by equation (15). The excellent agreement between the experimental results and those theoretically calculated by means of the reduced quantum trajectories shows the suitability of the latter in describing decoherence in interference phenomena. The dynamical behavior of neutrons within this approach is illustrated in Figure 1(b), where a sample of trajectories associated to the results in Figure 1(a) is displayed. From this plot it is apparent that, after the wave packets get close enough (at a distance of 1 m from the two slits, approximately), some trajectories (mainly those closer to the symmetry axis of the experiment) begin to show the typical "wiggling" behavior characterizing true Bohmian trajectories in interference processes with no decoherence [14]. Obviously, this behavior is more attenuated in both space and time than in the case of true Bohmian trajectories (without decoherence) because of the interference damping; in space because interference effects are relevant only for the central channels, as can be seen in Figure 1(a), and in time because $t_f > \tau_c$.

In Figure 2 the two limit cases of coherence for this model are illustrated: (a) total coherence ($\tau_c = \infty$) and (b) null coherence ($\tau_c = 0$). Similar to Figure 1, the statistical results obtained by means of reduced quantum trajectories and SQM (left) as well as a sample of representative trajectories (right) are displayed. Notice that, despite null coherence (see Figure 2(b)), the trajectories do not cross the symmetry axis that separates the regions covered by each slit, as in the case of total coherence (see Figure 2(a)). This is a manifestation of the contextual character of quantum trajectories, which remains even under these conditions. The absence of interference prevents the particles from undergoing the typical "wiggling" motion that leads to the different diffraction channels [14], but not from being non–locally correlated with particles coming from the other slit. Thus, within the approach proposed here we can see that decoherence leads to a suppression of quantum interference, but not to loss of memory on the initial context information (i.e., the existence of two slits). This is somehow similar to what happens in BM when trying to reach the classical limit without appealing to any decoherence mechanism [32]; classical–like statistical patterns emerge, but contextuality does not disappear.

According to the preceding statement, the structure of the reduced quantum trajectories allows to characterize different situations by their contextuality. That is, a situation where two slits are independently open can be easily distinguished from another where both are simultaneously open but there is total decoherence. These cases are illustrated in Figure 3. Although the trajectories started close to the outermost edges of each slit are identical in both cases, as the initial positions approach the innermost edges the behavior of the trajectories gets different. When the slits are independently open (see Figure 3(a)), each set of trajectories is associated to an independent wave, and the crossing between trajectories coming from different slits is allowed because their dynamics are totally uncoupled. On the contrary, when the two slits are simultaneously open (see Figure 3(b)), the dynamics are still strongly coupled, leading to an apparent "repulsion" between both sets of trajectories as they meet at about $z \approx 1$ m. Note that this effect can only be detected by means of the trajectories, since the measured intensity does not reveal any clue about it; in both cases it is a sum of the probabilities associated to each slit, as given by equation (20). Of course, true Bohmian trajectories would show that this non–crossing takes place in the $3(N+1)$–dimensional

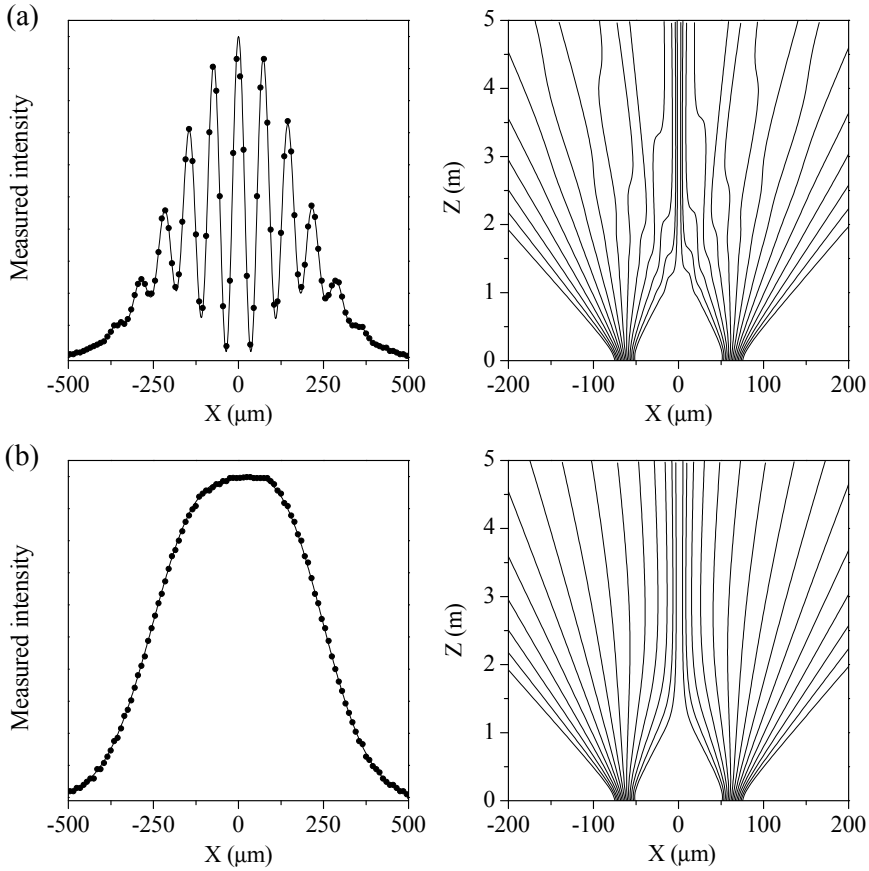


**Fig. 2.** Left: Intensity obtained from quantum trajectories (•) and SQM (full line) for: (a) total coherence ($\tau_c = \infty$) and (b) null coherence ($\tau_c = 0$). Right: Samples of trajectories illustrating the dynamics of the results shown in the left part.

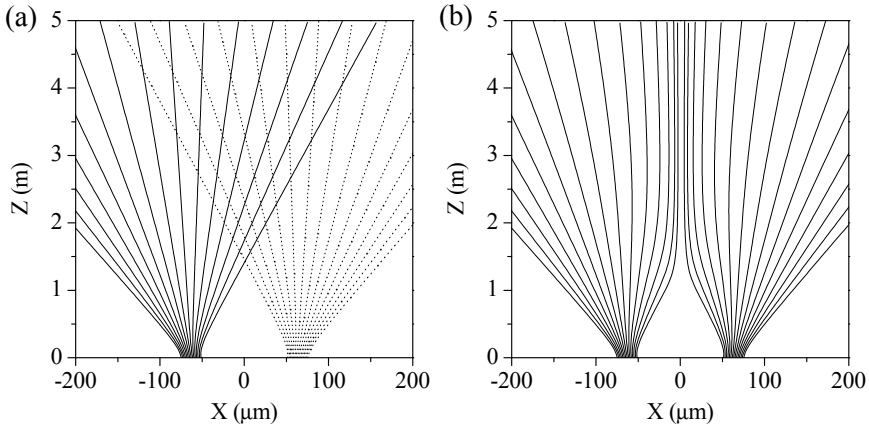


**Fig. 3.** Quantum trajectories for two different contexts: (a) slits independently open and (b) slits simultaneously open with $\tau_c = 0$.

configuration space where the system–plus–environment is described.

## 4 Conclusions

Realistic simulation of system–plus–environment interactions from purely quantum–mechanical approaches constitutes a hard computational task due to the many degrees of freedom involved. Nonetheless, it has become a topic of mayor interest in recent years [24] because of its important in different fields in physics, chemistry, and biology. Here we have proposed a quantum trajectory description, based on BM, that allows to study such problems without taking into account explicitly the evolution of the environment degrees of freedom. For that, the trajectories are directly obtained from the system reduced density matrix, with the action of the environment arising from a damping term that appears in such reduced density matrix. In this way, these trajectories reduce computational efforts as well as provide a physical inside on the physics taking place in phenomena where the system coherence is lost because of environment effects.

To illustrate the feasibility of our trajectory approach, we have applied it to the problem of decoherence in interference phenomena, in particular, to the disappearance

of interferences in the double–slit experiment. With this model it is shown that, effectively, interference fringes disappear, although the trajectory dynamics is still influenced by both slits, despite what one would expect. This is because the trajectory dynamics is constrained to the system reduced subspace instead of the full system–plus–environment configuration space, from which one can see that the projection of the system degrees of freedom onto the system subspace violates the non–crossing property of BM. Furthermore, based on this fact, we have also shown that the reduced trajectories can be used to distinguish between experiments that give identical SQM results. This is the case, for example, of an experiment performed with each slit independently open and another with both slits simultaneously open but total decoherence.

## Acknowledgements

This work has been supported by Ministerio de Educación y Ciencia (Spain) under projects MTM2006–15533, CONSOLIDER 2006–32, and FIS2004–02461; Comunidad de Madrid under the project S–0505/ESP–0158; and Agencia Española de Cooperación Internacional under the project A/6072/06. A.S. Sanz would also like to thank the Ministerio de Educación y Ciencia for a "Juan de la Cierva" Contract.

## References

1. R. Omnès R, Rev. Mod. Phys. **64**, 339 (1992).
2. W.H. Zurek, *Physics Today* **44**(10), 36 (1991).
3. D. Giulini, E. Joos, C. Kiefer, J. Kupsch, I.-O. Stamatescu, and H.D. Zeh, *Decoherence and the Appearance of a Classical World in Quantum Theory* (Springer, Berlin, 1996).
4. C. Kiefer and E. Joos, *Decoherence: Concepts and Examples*, in *Quantum Future*, eds. P. Blanchard and A. Jadczyk (Springer, Berlin, 1998).
5. E. Joos and H.D. Zeh, Zeit. Phys. **59B**, 223 (1985).
6. M.A. Nielsen and I.L. Chuang, *Quantum Computation and Quantum Information* (Cambridge University Press, Cambridge, 2000).
7. W.G. Unruh, Phys. Rev. A **51**, 992 (1995); R. Landauer, Phys. Lett. A **217**, 188 (1996); S. Mancini and R. Bonifacio, Phys. Rev. A **63**, 032310 (2001).
8. D. Bohm, Phys. Rev. **85**, 166, 180 (1952).
9. P.R. Holland, *The Quantum Theory of Motion* (Cambridge University Press, Cambridge, 1993).
10. A.S. Sanz, F. Borondo, and S. Miret–Artés, Phys. Rev. B **61**, 7743 (2000).
11. C. Philippidis, C. Dewdney, and B.J. Hiley, Nuovo Cimento B **52**, 15 (1979); C. Philippidis, D. Bohm, and R.D. Kaye, Nuovo Cimento B **71**, 75 (1982).
12. H.M. Wiseman, Phys. Rev. A **58**, 1740 (1998).
13. P. Ghose, A.S. Majumdar, S. Guha, and J. Sau Phys. Lett. A **290**, 205 (2001).
14. A.S. Sanz, F. Borondo, and S. Miret–Artés, J. Phys.: Condens. Matter **14**, 6109 (2002).
15. R. Guantes, A.S. Sanz, J. Margalef–Roig, and Miret–Artés Surf. Sci. Rep. **53**, 199 (2004).
16. E. Guay and L. Marchildon, *Preprint* quant-ph/0407077 (2004).
17. H.-P. Breuer and F. Petruccione, *The Theory of Open Quantum Systems* (Oxford University Press, Oxford, 2002).
18. W.K. Wootters and W.H. Zurek, Phys. Rev. D **19**, 473 (1979); R. Bhandari, Phys. Rev. Lett. **69**, 3720 (1992); B.-G. Englert, Phys. Rev. Lett. **77**, 2154 (1996); H.M. Wiseman, F.E. Harrison, M.J. Collet, S.M. Tan, D.F. Walls, and R.B. Killip, Phys. Rev. A **56**, 55 (1997); G. Björk and A. Karlsson, Phys. Rev. A **58**, 3477 (1998); S. Dürr, Phys. Rev. A **64**, 042113 (2001).
19. S. Dürr, T. Nonn, and G. Rempe, Phys. Rev. Lett. **81**, 5705 (1998).
20. A. Zeilinger, R. Gähler, C.G. Shull, W. Treimer, and W. Mampe, Rev. Mod. Phys. **60**, 1067 (1988).
21. D.M. Appleby, Found. Phys. **29**, 1885 (1999).
22. V. Viale, M. Vicari, and N. Zanghì Phys. Rev. A **68**, 063610 (2003).
23. A.S. Sanz, F. Borondo, and M. Bastiaans, Phys. Rev. A. **71** 42103 (2005).
24. D. Micha and I. Burghardt (eds.) *Quantum Dynamics of Complex Molecular Systems* (Springer, Berlin, 2006).
25. (a) W.H. Miller, J. Chem. Phys. **53**, 3578 (1970); (b) W.H. Miller, Faraday Discuss. **110**, 1 (1998); (c) R. Gelabert, X. Giménez, M. Thoss, H. Wang, and W.H. Miller, J. Phys. Chem. A **104**, 10321 (2000); (d) R. Gelabert, X. Giménez, M. Thoss, H. Wang, and W.H. Miller, J. Chem. Phys. **114**, 2562 (2001); (e) R. Gelabert, X. Giménez, M. Thoss, H. Wang, and W.H. Miller, J. Chem. Phys. **114**, 2572 (2001); (f) S. Zhang and E. Pollak, J. Chem. Phys. **121**, 3384 (2004); (g) S. Sengupta, E. Pollak, and S. Miret–Artés (to be published).
26. R.P. Feynman, Rev. Mod. Phys. **20**, 367 (1948); R.P. Feynman, A.R. Hibbs, *Quantum Mechanics and Path Integrals* (McGraw–Hill, New York, 1965).
27. P. Pechukas and U. Weiss (eds.), *Quantum Dynamics of Open Systems*, special issue in Chem. Phys. **268** (2001).
28. I. Percival, *Quantum State Diffusion* (Cambridge University Press, Cambridge, 1998).
29. R. Omnès, Phys. Rev. A **56**, 3383 (1997).
30. C.M. Savage and D.F. Walls, Phys. Rev. A **32**, 2316, 3487 (1985).
31. T. Qureshi and A. Venugopalan, Int. J. Mod. Phys. (to appear, 2007); *Preprint* quant-ph/0602052.
32. A.S. Sanz, F. Borondo, and S. Miret–Artés Europhys. Lett. **55**, 303 (2002).